



Acylation of anisole over 12-heteropolyacid of tungsten and molybdenum promoted zirconia

K.M. Parida*, Sujata Mallick, G.C. Pradhan

Colloids and Materials Chemistry Department, Institute of Minerals and Materials Technology, Bhubaneswar 751013, Orissa, India

ARTICLE INFO

Article history:

Received 13 February 2008
Received in revised form
11 September 2008
Accepted 11 September 2008
Available online 25 September 2008

Keywords:

Zirconia
12-Heteropoly acids of Mo and W
Acylation
Anisole

ABSTRACT

The liquid-phase acylation of anisole using acetic anhydride was performed over 12 heteropoly acid of tungsten and molybdenum (PWM) modified zirconia (ZPWM). Catalysts with different PWM loadings (3–20 wt.%) were prepared by the incipient wetness impregnation method using mesoporous zirconia and 12-heteropolyacid of W and Mo. The samples calcined at 500 °C were characterized by chemical analysis, nitrogen adsorption–desorption, surface acid sites, powder X-ray diffraction patterns, Fourier transform infrared spectroscopy, UV–vis diffuse reflectance spectroscopy, ³¹P nuclear magnetic resonance spectroscopy and electron probe microanalysis. The sample promoted by 15 wt.% PWM was found to be the most active in the acylation reaction giving 89% conversion with 97% para-selectivity. The effect of temperature, molar ratio and catalyst amount on the conversion of acetic anhydride and anisole were studied in detail to optimize the process parameters. Reusability of the catalyst was also appraised.

© 2008 Elsevier B.V. All rights reserved.

1. Introduction

Acylation reactions are largely employed in fine chemical industry to produce a variety of synthetic fragrances and pharmaceuticals [1–3]. The acylation of aromatics has been generally carried out with homogeneous Lewis acid-type catalysts (anhydrous metal halides such as AlCl₃ and FeCl₃) and acyl halides as acylating agents [4–6]. The overall process produces a significant amount of undesirable products and destroys the catalyst. The use of solid acids such as zeolites, sulfated zirconia, ZSM-5, Ga-doped SBA-15, mesoporous aluminosilicates synthesized from zeolite seeds etc. [7–11] represents an attractive alternative route with economic and environmental advantages. Among these catalysts, zeolites with shape selectivity are the most widely studied due to their strong and well-documented acid properties.

The Keggin-type heteropoly acids typically represented by the formula H_{8-x}[XM₁₂O₄₀] where X is the hetero atom, x is its oxidation state, and M is the addenda atom (usually Mo⁶⁺ or W⁶⁺), are the most important solid acid catalysis [12]. The HPAs like H₃PW₁₂O₄₀, H₃PMo₁₂O₄₀, H₄SiW₁₂O₄₀ and H₄SiMo₁₂O₄₀ have been widely used as acid and oxidation catalysts in the neat or supported form for organic synthesis [13,14]. We have also published a number of papers using these materials [15,16]. However, only a few studies on the use of 12-heteropoly acids of W and Mo have been reported [17].

In the present work, we have studied acylation of anisole using acetic anhydride over 12-heteropoly acid of molybdenum and tungsten modified zirconia. The characterizations of the modified catalysts have also been co-related with the catalytic activity.

2. Materials and methods

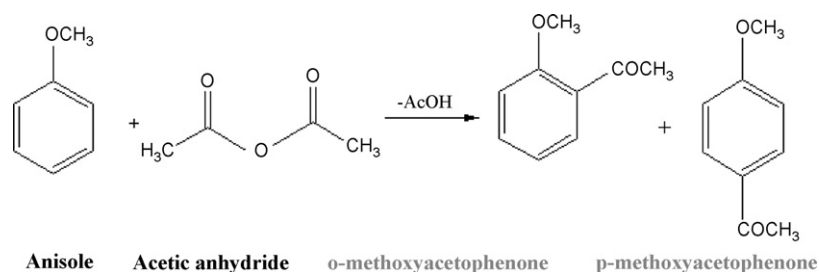
2.1. Preparation of zirconia

Zirconium hydroxide gel was prepared from aqueous solution of zirconium oxychloride (Fine Chemical) by dropwise addition of ammonium hydroxide solution (25% ammonia) (Merck) till it attained pH 9.5. The hydrogel was refluxed for 24 h, filtered and washed with deionized water and dried in an oven at 120 °C for 24 h. The finely grounded sample was calcined at 500 °C for 5 h (named Z hereafter).

2.2. Preparation of 12-heteropoly acids of tungsten and molybdenum

Na₂WO₄·2H₂O (45.1 g), Na₂MoO₄·2H₂O (33 g) and Na₂HPO₄·2H₂O (8.15 g) were dissolved in 200 ml of deionized water. The solution was kept at 80 °C for 3 h with agitation and then concentrated to 80 ml by the use of an evaporator. Then 100 ml of 24% HCl was added to it. The yellow crystals were obtained by extraction with ether from a 50% aqueous solution. The contents of P, Mo and W in PWM were analyzed by inductively coupled plasma (ICP) and found to be in the ratio 1:6:6.

* Corresponding author. Tel.: +91 674 2581636x425; fax: +91 674 2581637.
E-mail address: kmparida@yahoo.com (K.M. Parida).



Scheme 1. Schematic representation acylation of anisole.

2.3. Preparation of catalyst

A series of catalysts with 3–20 wt.% loading was synthesized by impregnating 2 g of Z with an aqueous solution of 12-heteropoly acid of tungsten and molybdenum (PWM) (0.06 g to 0.30 g/10–50 ml of conductivity water) under constant stirring followed by heating till complete evaporation of water takes place (4 h). Then it was dried in an oven at 110 °C for 24 h. Catalysts with different PWM loading from 3 to 20 wt.% were then calcined at 500 °C. The catalysts will be hereafter referred to as xZPWM ($x = 3\text{--}20$ wt.%).

2.4. Physico-chemical characterization

The BET surface area and pore size distribution were determined by multipoint N_2 adsorption–desorption method at liquid N_2 temperature (-196 °C) by a Sorptomatic 1990 instrument (ThermoQuest, Italy). Prior to analyses, all the samples were subjected to vacuum at 200 °C to ensure a clean surface.

Surface acidity was determined spectrophotometrically on the basis of irreversible adsorption of organic bases such as pyridine (PY, $pK_b = 3.5$) and 2, 6-dimethyl pyridine (DYPY, $pK_b = 8.7$) [18].

The X-ray powdered diffraction pattern was recorded on a Philips PW 1710 diffractometer with automatic control. The patterns were run with a monochromatic CuK_{α} radiation at a scan rate of 2° min^{-1} .

The FTIR spectra were taken using a Jasco FTIR 5300 spectrometer in KBr matrix in the range of $400\text{--}4000 \text{ cm}^{-1}$.

The UV–vis spectra of the samples were recorded in a Varian UV–vis-DRS spectrophotometer fitted with Carry 100 software. The spectra were recorded against the boric acid background.

The ^{31}P NMR spectra were recorded on a Varian Mercury 300 MHz NMR spectrometer, ^{31}P chemical shifts are referenced to 85% H_3PO_4 as an external standard, and the time of scan was 380.

Micrographs showing X-ray image mapping of different elements of 12-heteropoly acid of tungsten and molybdenum supported zirconia were taken using a Japanese Model (JXA-8100) EPMA.

2.5. Catalytic activity towards acylation of anisole

The acylation reaction was carried out in liquid phase in a 50 ml three-necked round bottom flask fitted with a thermometer, reflux condenser with $CaCl_2$ tube and a magnetic stirrer bar. A mixture of 100 mmol of anisole and 10 mmol of acetic anhydride were added to the flask along with 0.1 g of n-tridecane, which was used as an internal standard for GC analysis. The catalyst was added after adjusting the temperature to 70 °C. The reaction mixture was separated from the catalyst after 2 h and analyzed gas chromatographically, using capillary column (Scheme 1).

Addition of p- and o-methoxyacetophenone to the reaction mixture was done to know the influence of the product on conversion

and selectivity. To confirm the active species as solid acids, the reaction filtrate was tested for the presence of metal ions. Standards containing 1–6 wt.% PMA in water were prepared. To 10 ml of the solution 1 ml of 10% ascorbic acid was added. Then it was diluted to 25 ml. The resultant blue coloured solution was scanned at $\lambda_{\text{max}} 784 \text{ cm}^{-1}$. A standard calibration curve was obtained by plotting values of absorbance with percentage solution. About 1 g of 12 wt.% ZPWM with 25 ml n-butanol was refluxed for 4 h. Then 10 ml of the superintendent solution was treated with 10% ascorbic acid. The same procedure was repeated with the filtrate of the reaction mixture after completion of the reaction.

3. Results and discussion

3.1. Characterization

Table 1 shows the BET surface area of zirconia and ZPWM with different weight percentages. Surface area of zirconia is found to be $142 \text{ m}^2/\text{g}$. With the increase in PWM loading from 0 to 15 wt.%, the surface area increases from 142 to $291 \text{ m}^2/\text{g}$. However with further increase in PWM beyond 15 wt.%, the surface area decreases. This implies that the presence of PWM plays a role in making the material porous. The added PWM forms a surface overlayer that reduces the surface diffusion of zirconia and inhibits sintering. It stabilizes the tetragonal phase of zirconia, which leads to an increase in surface area (cf. XRD pattern). However, when the PWM content increases beyond 15 wt.%, pore blocking takes place due to the presence of an excess amount of 12-heteropoly acids of molybdenum and tungsten.

Table 1
Surface area of various catalysts.

Catalysts	Surface area ($\text{m}^2 \text{ g}^{-1}$)
Z	142
3 ZPWM	156
6 ZPWM	176
9 ZPWM	189
12 ZPWM	211
15 ZPWM	254
20 ZPWM	239

Table 2
Acid sites of various catalysts.

Catalysts	Acid sites ($\mu\text{mol/g}$)	
	PY	2,6 DMPY
3 ZPWM	121	43
6 ZPWM	154	54
9 ZPWM	167	72
12 ZPWM	199	86
15 ZPWM	243	106
20 ZPWM	225	95

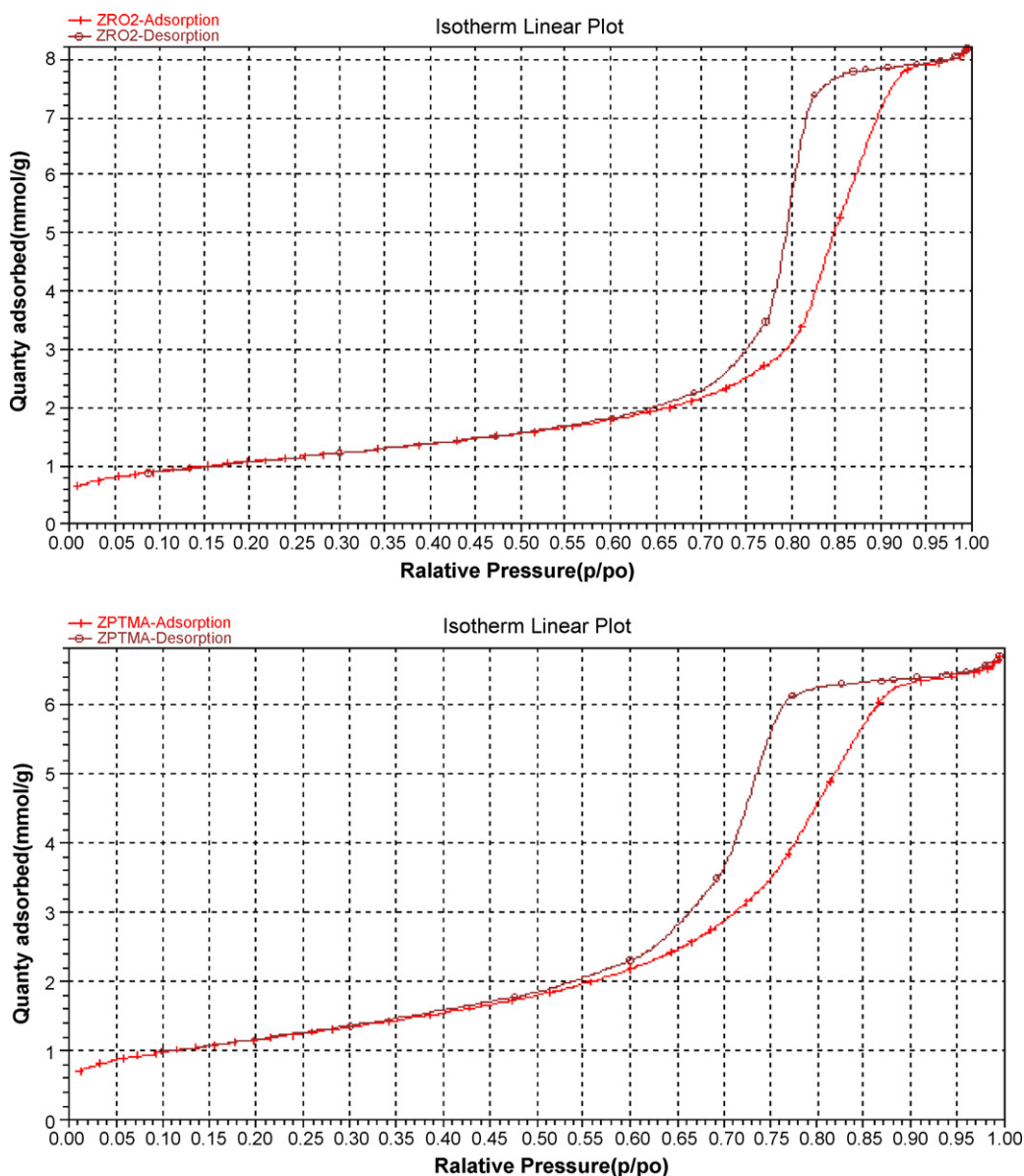


Fig. 1. (a) N₂ adsorption–desorption isotherm of zirconia. (b) N₂ adsorption–desorption isotherms of 12-heteropoly acid of W and Mo supported on zirconia.

Table 2 shows the surface acid sites of zirconia and zirconia impregnated PWM samples. Adsorption of pyridine (PY) measures the total acidity where as 2,6-dimethylpyridine (DMPY) gives Brønsted acid sites. It is found that with an increase in the PWM content from 0 to 15 wt.%, the acidity gradually increases from 156 to 310 $\mu\text{mol/g}$, and thereafter decreases to 276 $\mu\text{mol/g}$ for 20 wt.% ZPWM. The increase in surface acidity, with an increase in PWM loading may be due to the formation of monolayer coverage of PWM on zirconia. The decrease in surface acidity at high PWM concentration is probably due to the formation of multilayer coverage of PWM on zirconia, which decreases the number of Brønsted acid sites and consequently that of total strong acid sites.

The nitrogen adsorption–desorption isotherms of parent zirconia and 15 wt.% ZPWM are shown in Fig. 1a and b. The isotherms are of the type IV isotherm according to the IUPAC classification of adsorption isotherms [19], which is a typical characteristic of mesoporous solids. Inflections at P/P_0 0.7–1.0 for zirconia and at 0.8–1.0 for 15 wt.% ZPWM are seen in the figure; these are ascribed to the spontaneous filling of mesopores due to capillary condensation.

Fig. 2 shows the BJH pore size distribution of zirconia and 15 wt.% ZPWM. From the figure one can see that there is no appreciable difference in pore diameter between zirconia and 15 wt.% ZPWM.

The XRD patterns of zirconia and ZPWM samples are presented in Fig. 3. It was observed that pure zirconia contains a mixture of tetragonal and monoclinic phases with the latter as the major constituents. However, XRD of samples with low PWM loadings is similar to that of the support. As percentage loading of PWM increases, it shows increase in the tetragonal phase while at 15 wt.% loading ZPWM is fully tetragonal. But on further increase in PWM loading, it shows the monoclinic phase along with the tetragonal one.

The FTIR spectra of zirconia and zirconia impregnated with 12-heteropoly acid of tungsten and molybdenum (15 wt.% ZPWM) are presented in Fig. 4a and b. The FTIR spectrum of zirconia shows a broad band in the region of 3410 cm^{-1} due to asymmetric stretching of OH group and two bands at 1621 and 1386 cm^{-1} which are due to bending vibration of $-(\text{H}-\text{O}-\text{H})-$ and $-(\text{O}-\text{H}-\text{O})-$ bond. The band at 503 cm^{-1} resulted from the existence of both tetragonal and

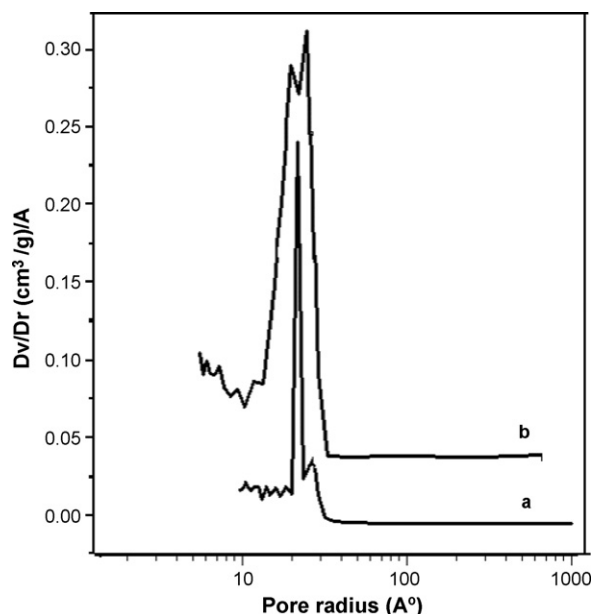


Fig. 2. Distribution of pore size as a function of pore radius of (a) zirconia and (b) 20 wt.% ZPWM.

monoclinic zirconia. The spectra at 580 and 730 cm^{-1} are attributed to the presence of the Zr-O bond (Fig. 5a). In addition to these bands, the FTIR spectra of 3–20 wt.% of ZPWM samples show bands at 1072, 972, 877 and 790 cm^{-1} due to PWM Keggin species. The FTIR spectrum of 15 wt.% ZPWM is shown as an example (Fig. 4b). The characteristic bands found at 1068, 890, 792 cm^{-1} are assigned to the symmetric stretching of P-O, M-O_c-Mo, and M-O_e-M respectively and a weak shoulder at 962 cm^{-1} due to M-O_t confirmed the presence of the undegraded 12-heteropoly acid of tungsten and molybdenum. Here t stands for the terminal oxygen bonding to one

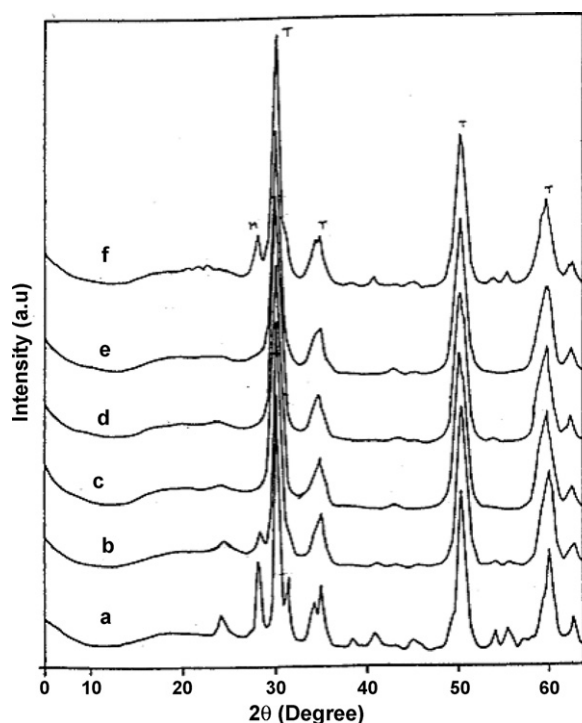


Fig. 3. XRD patterns of (a) Z, (b) 9 wt.% ZPWM, (c) 12 wt.% ZPWM, (d) 15 wt.% ZPWM, (e) 20 wt.% ZPWM and (f) 25 wt.% ZPWM (calcined at 500 °C).

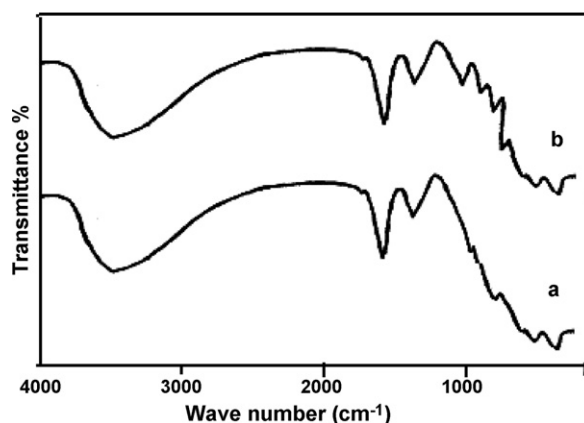


Fig. 4. FTIR spectra of (a) Z and (b) 20 wt.% ZPWM.

M atom, c for the corner sharing oxygen atom connecting M_3O_{13} units and e for the edge sharing oxygen connecting Ms.

Fig. 5 shows the background subtracted UV-vis-DRS spectra of (a) zirconia, (b) 15 wt.% ZPWM calcined at 500 °C. The zirconia sample (Fig. 5a) exhibits a strong absorption band at 230 nm, which may be attributed to the charge transfer from oxide species to zirconium cation ($\text{O}^- \rightarrow \text{Zr}^{4+}$). In contrast, the spectra of 15 wt.% ZPWM broad showing bands at 220 nm and 265 nm match well with the literature [20], suggesting thereby the presence of undegraded $\text{H}_3\text{PW}_6\text{M}_6\text{O}_{40}$ species.

The ^{31}P chemical shift (δ) provides important information concerning the structure, composition and electronic states of HPA. The crystal of $\text{H}_3\text{PW}_6\text{M}_6\text{O}_{40}$ has the Keggin structure based on a central PO_4 tetrahedron surrounded by 12 MO_6 octahedral M_3O_{13} group. The groups of M_3O_{13} are linked by sharing corners to each other and to the central PO_4 tetrahedron. Mo and W are crystallographically disordered, each $\text{M} = 1/2\text{Mo} + 1/2\text{W}$, statistically occupying in the crystal.

The ^{31}P NMR spectrum of $\text{H}_3\text{PW}_6\text{M}_6\text{O}_{40}$ exhibits a single line at -1.3 ppm due to the P-O bond (Fig. 6a). In the case of $\text{H}_3\text{PW}_6\text{M}_6\text{O}_{40}$

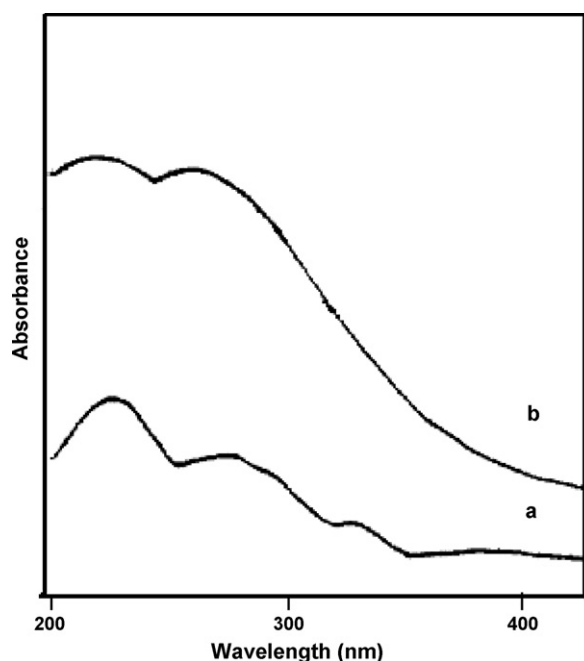


Fig. 5. UV-vis spectra of (a) Z and (b) 20 wt.% ZPWM.

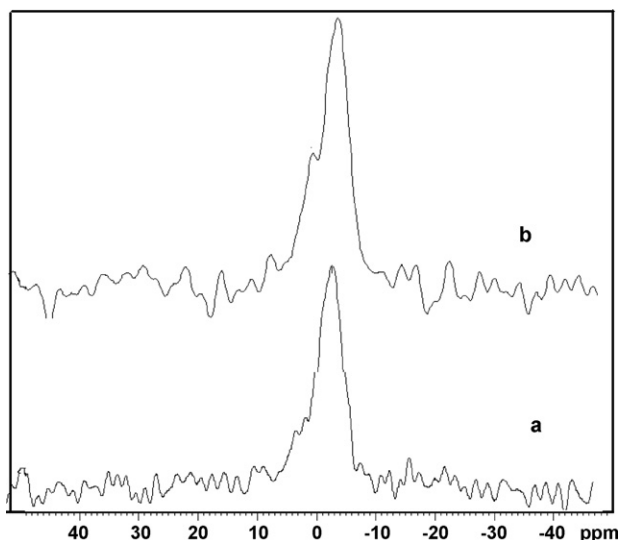


Fig. 6. ^{31}P NMR spectra of (a) $\text{H}_3\text{PMo}_6\text{W}_6\text{O}_{40}$ and (b) 20 wt.% ZPWM.

loaded zirconia catalyst the chemical shift occurred at -1.3 ppm suggesting the presence of undegraded $\text{H}_3\text{PW}_6\text{M}_6\text{O}_{40}$.

Electron micrographs of zirconia and 15 wt.% ZPWM samples are presented in Figs. 7 and 8, showing the secondary electron image of haphazardly arranged zirconia crystallites and zirconia supported 12-heteropoly acid of W and Mo.

Fig. 9 illustrates the X-ray image maps of W, Mo, P, and Zr elements in a selected area (SL) showing their level of concentration through clustering of pixels. It is found that W and Mo are adsorbed in Zr grain more than that of phosphorus. This is obvious since in original PWM, the tungsten and molybdenum contents are 6 times higher than the phosphorus one.

3.2. Acylation of anisole

The acylation of anisole with acetic anhydride gave ortho-methoxyacetophenone and para-methoxyacetophenone as the acylated products. The conversion is expressed as the percentage of acetic anhydride converted into the acylated product. In order to investigate the effect of 12-heteropoly acids of molybdenum and

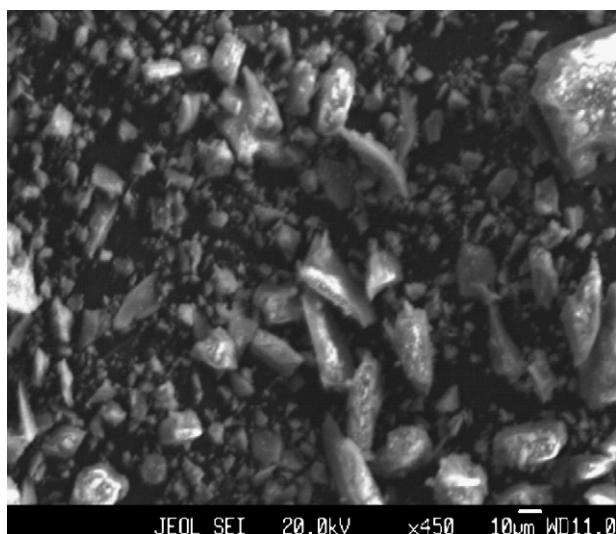


Fig. 7. Scanning electron micrograph of zirconia.

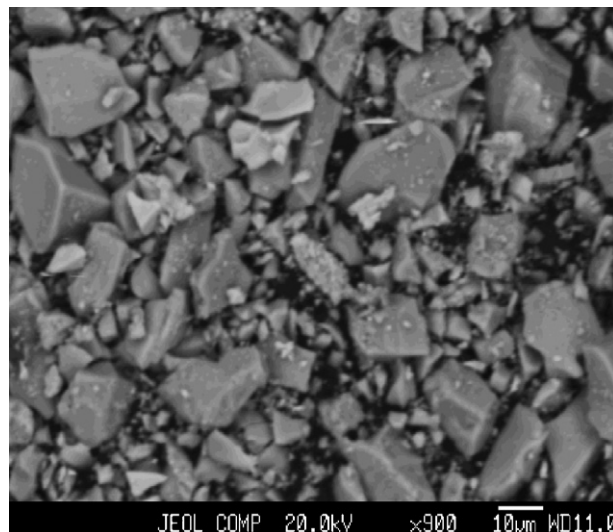


Fig. 8. Scanning electron micrograph of 20 wt.% ZPWM.

tungsten loadings, 3–20 wt.% ZPWM catalysts are used in acylation of anisole with acetic anhydride at 70°C . The results show that all the catalysts were efficient for catalyzing the reaction. The selectivity of para- and ortho-methoxyacetophenone is shown in Table 3. Among the catalysts with different PWM loadings, the 15 wt.% ZPWM catalyst gave the highest conversion (89%). Further, increase in the PWM loading decreases the acetic anhydride conversion. The activity of the catalysts has been found to be related to the number of Brønsted acid sites. The correlation of catalytic activities with number of acid sites and strength of Brønsted acid sites have been reported by Gauthier et al. [21]. Since no metal ion was present in the reaction filtrate, it is presumed that the true active species is the solid acid, which developed due to chemical interaction between the HPA and zirconia. This also supports that the catalyst is stable under reaction conditions.

Anisole is an ortho/para directing substrate for electrophilic substitution reactions, presenting a relatively high susceptibility to such reactions by means of the release of electron from the methoxy-oxygen atom to the aromatic ring, constituting itself a very feasible substrate for the synthesis of substituted ketones. For the acylation of anisole by acetic anhydride, Corma et al. [22] have suggested that an acylium cation is formed by the protonation of an acyl species interacting with the proton of the zeolite, and that the acylium species attaches to the nucleophilic aromatic ring to form the acylated product. On the contrary Bonati et al. [23] have suggested that the acylating agent is ketene, which is formed in situ by the decomposition of acetic anhydride into acetic acid and ketene. The electrophilic ketene then reacts with the anisole in a

Table 3

Conversion and selectivity of various catalysts towards acylation of anisole.

Catalyst	Conversion (%)	Selectivity	
		p-MAP	o-MAP
Z	45	79	21
3 ZPWM	57	82	18
6 ZPWM	65	85	15
9 ZPWM	74	89	11
12 ZPWM	83	92	8
15 ZPWM	89	97	3
20 ZPWM	72	93	7

Anisole: 100 mmol, acetic anhydride: 10 mmol, catalyst amount: 0.1 g, temperature: 70°C , and time: 2 h.

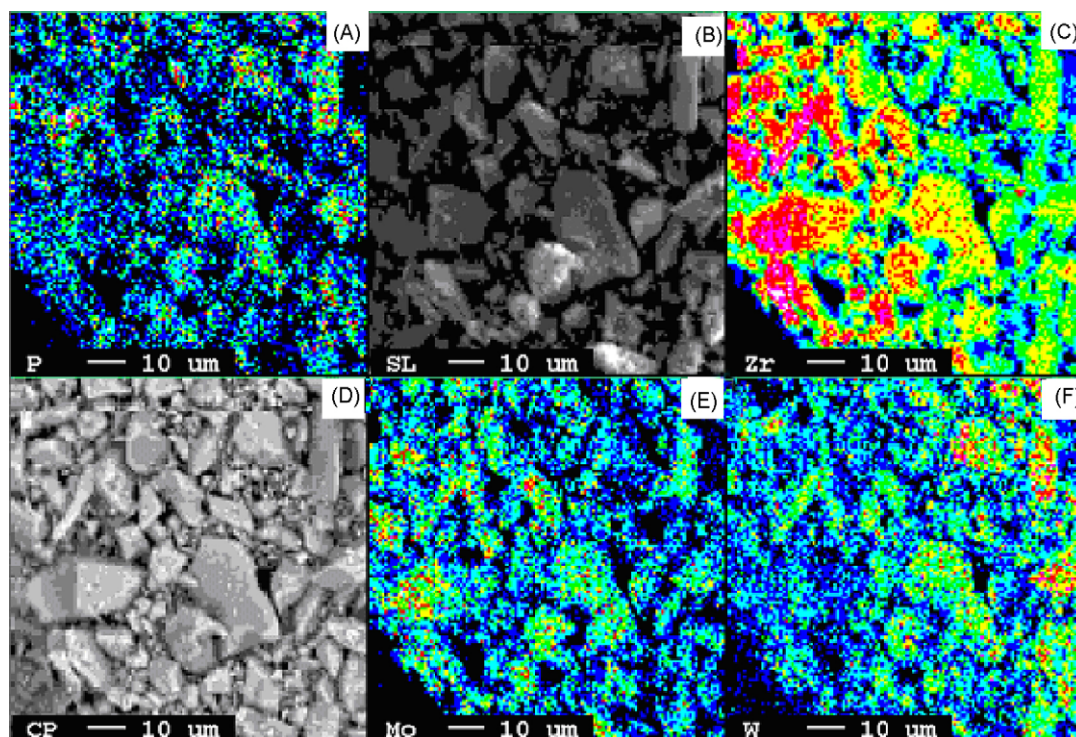
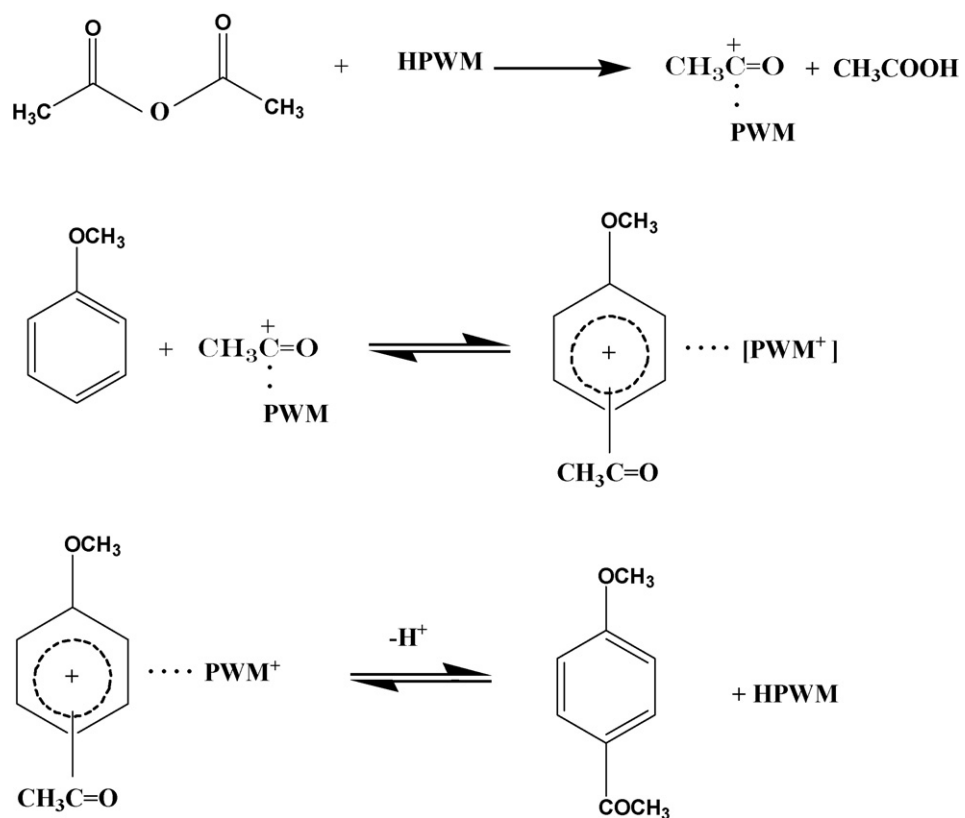


Fig. 9. Scanning electron micrograph of 20 wt.% ZPWM (A) X-ray image map of Si, (B) Secondary electron image of morphological view of 20 wt.% ZPWM, (C) X-ray image map of Zr, (D) Morphological view of 20 wt.% ZPWM, (E) X-ray image map of Mo, and (F) X-ray image map of W.



Scheme 2. Mechanism for acylation of anisole.

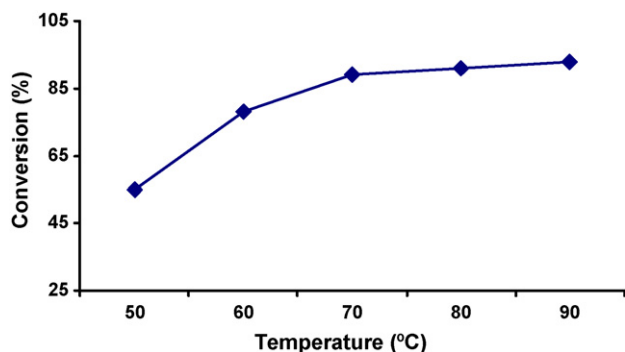


Fig. 10. Effect of reaction temperature on acylation of anisole. Catalyst amount 0.1 g, reaction temperature 70 °C, anisole: acetic anhydride ratio 10:1, time = 2 h.

rather similar manner to the acylium species. In this study the possible pathways for the production of methoxyacetophenones in the Friedel–Crafts acylation of anisole with acetic anhydride catalysed by heteropoly acids are shown below:

The interaction of anhydride molecule with Brønsted acid site of PWM acid generates acylium ion, which subsequently attacks the π -electrons of anisole to form methoxyacetophenones (Scheme 2).

3.2.1. Influence of reaction temperature

The influence of reaction temperature on the acylation of anisole is shown in Fig. 9. The reaction was carried out in the temperature region 50–90 °C over 15 wt.% ZPWM as catalyst with the other parameters fixed. At 50 °C, acetic anhydride conversion is 65% and it increases to 91% at 80 °C. Further increase in reaction temperature to 90 °C has no appreciable effect on the acetic anhydride conversion. Similar observation has also been made by Devassy et al. for benzoylation of veratrole with benzoic acid [24].

3.2.2. Influence of catalyst amount

The effect of the catalyst amount (0.05, 0.1, and 0.15 g) was investigated at an anisole-to-acetic anhydride mole ratio of 10:1 at 70 °C (Fig. 10). The conversion of anisole increases from 61 to 91% with an increase in the catalyst amount from 0.05 to 0.15 g.

3.2.3. Influence of molar ratio

The effect of molar ratio was studied at anisole-to-acetic anhydride ratios of 1:1, 5:1 and 10:1 at a temperature of 70 °C over 15 wt.% ZPWM catalyst and the results are shown in Fig. 11. The conversion was found to increase with an increase in the anisole-to-acetic anhydride molar ratio. At a molar ratio of 1, the conversion was 13% and with an increase in the molar ratio to 10, the con-

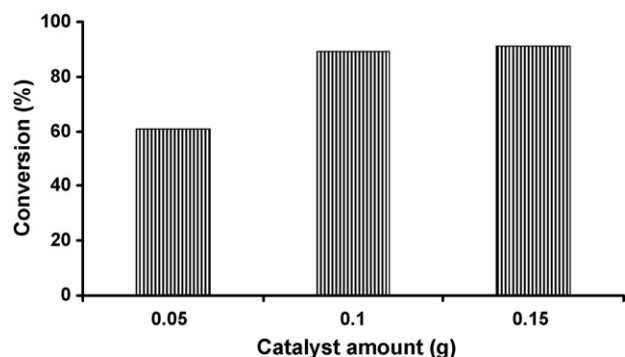


Fig. 11. Effect of catalyst amount on acylation of anisole. Reaction temperature 70 °C, anisole: acetic anhydride = 10:1, time = 2 h.

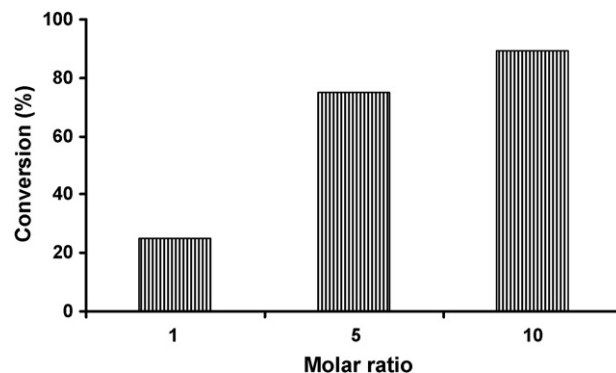


Fig. 12. Effect of molar ratio of anisole/acetic anhydride on acylation of anisole catalyst amount 0.1 g, reaction temperature 70 °C, time = 2 h.

version increased to 89%. It was observed that the conversion decreased by adding *p*- or *o*-methoxyacetophenone in the reaction mixture. This is probably due to the inhibiting effect of methoxyacetophenone, which can strongly adsorb on the catalyst surface. This inhibiting effect would be less significant for mixtures richer in anisole, because the excess of anisole acts as a solvent for the ketone produced, product inhibition reduced, and therefore the acetic anhydride conversion is higher at higher anisole-to-acetic anhydride molar ratios [25,26]. The inhibiting effect was also confirmed by *p*-methoxyacetophenone in the reaction mixture.

3.2.4. Influence of time

The effect of time on conversion and selectivity for *p*-methoxyacetophenone over 15 wt.% ZPTM is shown in Fig. 12. It was found that the percentage of conversion increased from 45 to 93% with an increase in reaction time from 0.5 to 3 h and then remains almost constant with further rise of reaction time up to 4 h.

3.3. Recyclability of the catalyst

The catalyst with 15 wt.% loading was used for recycling experiments. In order to regenerate the catalyst after 2 h of reaction, it was separated by filtration, washed several times with conductivity water and dried at 110 °C. The material calcined at 500 °C was used in the acylation of anisole with a fresh reaction mixture. In the regenerated sample after two cycles, the yield decreased by 3%. The activity loss observed with the regenerated catalyst could be due to partial loss of acid sites of the catalyst during reaction/regeneration (Fig. 13).

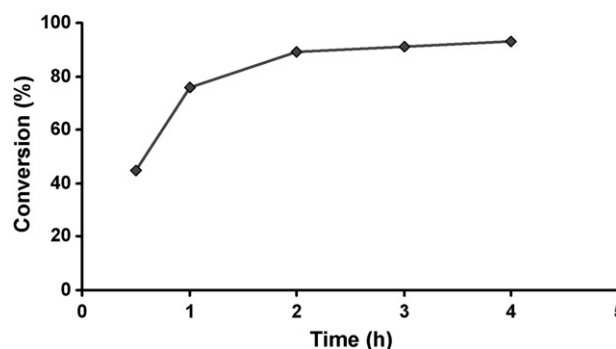


Fig. 13. Effect of reaction time on acylation of anisole. catalyst amount = 0.1 g, reaction temperature 70 °C anisole: acetic anhydride ratio 10:1.

4. Conclusions

Based on the above studies the following conclusions may be drawn:

- The 12 heteropoly acid of W and Mo supported on zirconia are found to be an efficient, stable and reusable solid acid catalyst towards anisole acylation reaction.
- The nitrogen adsorption–desorption studies have revealed that the catalyst retain the mesoporosity.
- There is no appreciable change in pore diameter after impregnation of heteropoly acid in zirconia.
- FTIR and ³¹P NMR spectra confirmed that the heteropoly acids of W and Mo retain their Keggin-type structure when supported on zirconia even at 500 °C.
- EPMA studies revealed that the dispersion of PWM anion into the surface of the support is uniform.
- The catalyst is good for the conversion of anisole (89%) to paramethoxyacetophenone (97%).
- This catalyst system is easy to prepare and the deactivated catalyst can be reused after regeneration by calcinations.
- PWN/ZrO₂ is an ecofriendly catalyst for use in acylation reactions.

Acknowledgements

The authors are thankful to Prof. B.K. Mishra, Director, Institute of Minerals and Materials Technology (CSIR), Bhubaneswar for the constant encouragement and permission to publish this paper. One of the authors Mrs. Sujata Mallick is grateful to CSIR for the award of SRF. The financial support from DST is acknowledged.

References

- [1] G.A. Olah, Friedel–Crafts Chemistry, Wiley, New York, 1973.

- [2] G. Franck, J.W. Stadelhofer, Industrial Aromatic Chemistry, Springer-Verlag, Berlin, 1988.
- [3] P.J. Harrington, E. Lodewijk, Org. Process Res. Dev. 1 (1997) 72–76.
- [4] P.H. Gore, in: G.A. Olah (Ed.), Friedel–Crafts and Related Reactions, vol. III, Wiley/Interscience, New York, 1964, pp. 64–72.
- [5] B.S. Furniss, A.J. Hannaford, P.W.G. Smith, A.R. Tatchell, Vogels Text Book of Practical Organic Chemistry, fifth ed., Longman, Singapore, 1989.
- [6] Kirk-Othmer, Encyclopedia of Chemical Technology, 24, fifth ed., 1997, pp. 38–51.
- [7] C. Guinard, V. Pedron, F. Richard, R. Jacquot, M. Spagnol, J.M. Coustard, G. Perot, Appl. Catal. A 234 (2002) 79–90.
- [8] M.J. Climent, A. Corma, H. Garcia, J. Primo, Appl. Catal. A: Gen. 49 (1989) 109–123.
- [9] L.G.A. van de Water, J.C. van der Waal, J.C. Jansen, T. Maschmeyer, J. Catal. 223 (2004) 170–178.
- [10] Z. El Berrichi, L. Cherif, O. Orsen, J. Fraissard, J.P. Tessonnier, E. Vanhaecke, B. Louis, M.J. Ledoux, C. Pham-Huu, Appl. Catal. A: Gen. 298 (2006) 194–202.
- [11] P.C. Shih, J.H. Wang, C.Y. Mou, Catal. Today 365 (2004) 93–95.
- [12] Y. Ono, J.M. Thomas, K.I. Zamarev (Eds.), Perspectives in Catalysis, Blackwell, London, 1992.
- [13] C.L. Hill (Ed.), Chem. Rev. 98 (1998) 1–2.
- [14] T. Okuhara, N. Mizuno, M. Misono, Adv. Catal. 41 (1996) 113–252.
- [15] Sujata Mallick, K.M. Parida, Catal. Commun. 8 (2007) 889–893.
- [16] K.M. Parida, Sujata Mallick, J. Mol. Catal. A: Chem. 275 (2007) 77–83.
- [17] Jun Peng, Yunshan Zhou, Enbo Wang, Yan Xing, Heng Q. Jia, J. Mol. Struct. 444 (1998) 213–219.
- [18] I.V. Kozhevnikov, Russ. Catal. Rev. Sci. Eng. 37 (1995) 311–352.
- [19] K.S.W. Sing, D.H. Everett, R.A.W. Haul, L. Moscou, R.A. Pierotti, J. Rouquerol, T. Siemieniowska, Pure Appl. Chem. 57 (1985) 603–619.
- [20] Yong Ding, B. Ma, Q. Gao, G. Li, L. Yan, J. Suo, J. Mol. Catal. A: Chem. 230 (2005) 121–128.
- [21] C. Gauthier, B. Chiche, A. Finiels, R. Geneste, J. Mol. Catal. A: Chem. 50 (1989) 219–229.
- [22] A. Corma, M.J. Climent, H. Garcia, J. Primo, Appl. Catal. A: Gen. 49 (1989) 109–123.
- [23] M.L.M. Bonati, R.W. Joyner, M. Stockenhuber, Catal. Today 81 (2003) 653–658.
- [24] M. Devassy Biju, S.B. Halligudi, J. Catal. 236 (2005) 313–323.
- [25] D. Rohan, C. Canaff, E. Fromentin, M. Guisnet, J. Catal. 177 (1998) 296–305.
- [26] P. Botella, A. Corma, J.M. Lopez-Nieto, S. Valencia, R. Jacquot, J. Catal. 195 (2000) 161–168.